Novel N-CNDs/PAni Modified Molecular Imprinted Polymer for Ultraselective and Sensitive Detection of Ciprofloxacin in Lentic Ecosystem: Dual Responsive Optical Sensor

TITLE

Komal Murugan[1], Abirami Natarajan[1*]

[1*]Department of Chemistry, Faculty of Engineering and Technology, SRM Institute of Science and Technology, Kattankulathur, Tamil Nadu-603 203, India.

*Corresponding author: e-mail: abiramin@srmist.edu.in

Supplementary figures

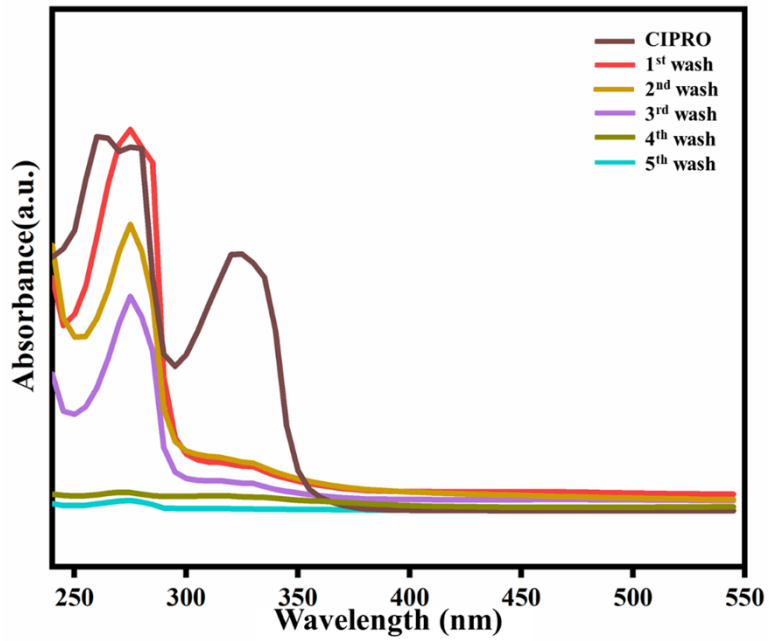

Figure S1. Elution of template (CIPRO) from N-CNDs/PAni/MIP.

Raman spectra interpretation:

Analyzing nanocomposite materials with Raman spectroscopy helps us understand structural disorder by revealing the nature and number of functional groups. The Raman spectra of N-CNDs/PAni/MIP (Fig. S2) show numerous bands that reveal the chemical composition. The notable band, exhibiting the most intense Raman signal at 1473 cm^{-1}, relates to the vibrational modes of C=N found in the quinoid rings of PAni [1]. In addition, the band seen at

1159 cm^{-1} corresponds to the C–H in-plane bending vibrations of the benzenoid rings in PANI [2]. Significantly, distinct vibrations for N-CNDs at 1378 cm^{-1} and 1589 cm^{-1} were also detected, linked to the defect band (D band) and graphite band (G band), respectively. The D band described vibrations of carbon atoms with suspended bands, while the G band related to sp^2-banded carbon atoms in a 2D hexagonal lattice. Significantly, the existence of a Raman band at 1019 cm^{-1}, which corresponds to the stretching vibration of Si-OH in APTES, indicates its contribution to the production of nanocomposite [4]. Overall, these results show that the N-CNDs/PAni/MIP nanocomposite was successfully synthesized and has an amorphous nature.

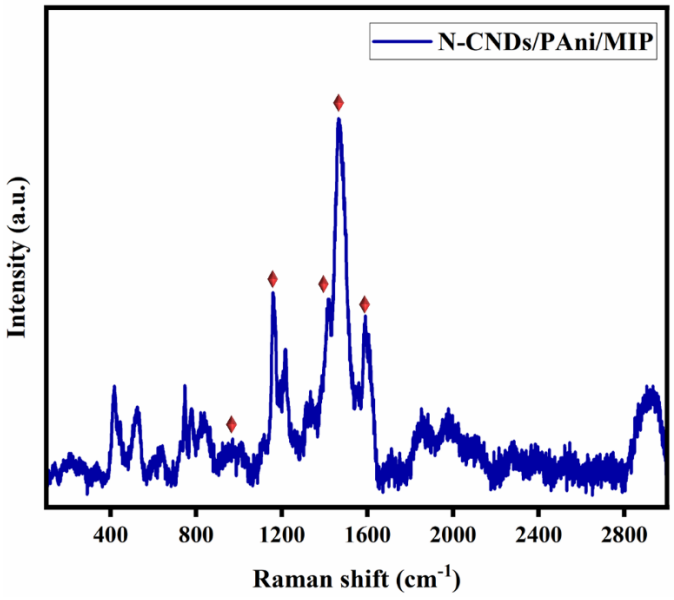

Figure. S2 Raman spectra of N-CNDs/PAni/MIP.

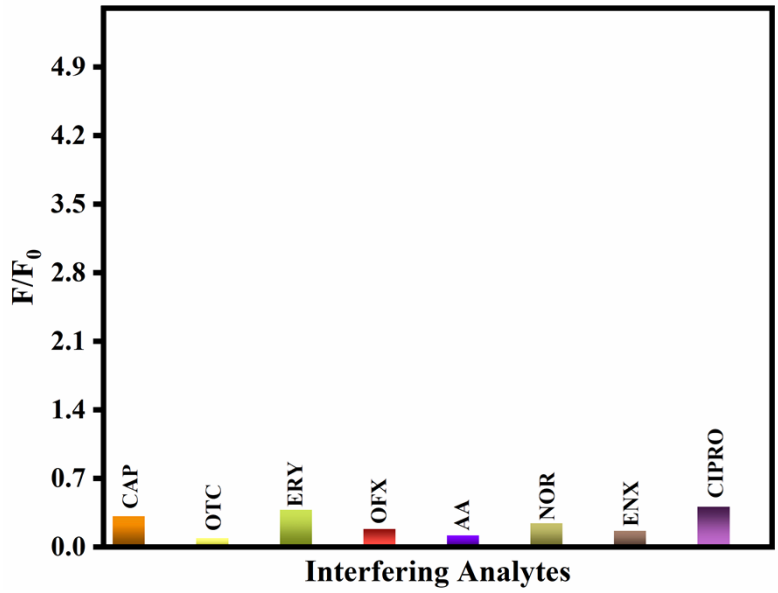

Figure S3. Fluorescence spectra of N-CNDs/PAni with different interfering analytes.

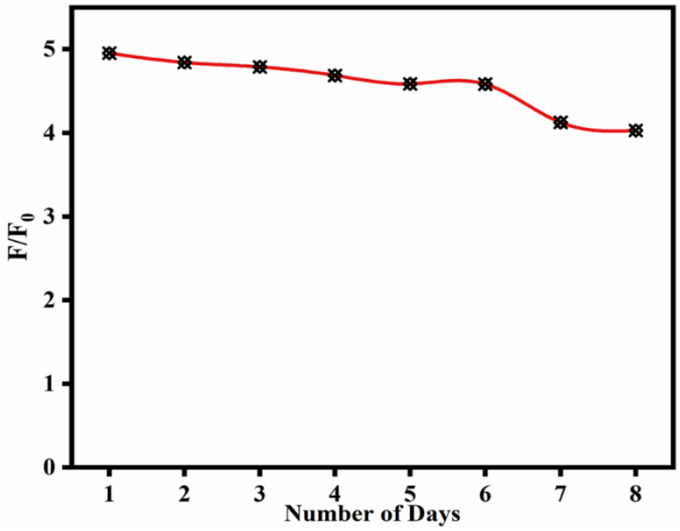

Figure S4. Stability of N-CNDs/PAni/MIP.

The reactive active species such as hydroxyl radical (•OH), hole (h^+), and superoxide anion (O^{2-}) play vital roles during the catalytic reactions. This study employed scavengers such as EDTA, IPA, and BQ to capture active species such as h^+, •OH, and $•O^{2-}$ that are involved in the catalytic process of N-CNDs/PAni/MIP. When any reactive species is generated during the reaction, the response signals are observed to decrease. Figure S5(a) illustrates that the inclusion of IPA resulted in a significant decrease in the absorption of the colorimetric reaction system. Conversely, the addition of BQ and EDTA had no noticeable impact on these parameters. The UV-Vis absorbance values are 0.7135, 0.689, 0.699, and 0.1165, respectively. These values correlate to the absence of scavengers and the presence of different scavengers ($•O^{2-}$, h^+, and •OH). This confirms that the nature of peroxidase-like activity in N-CNDs/PAni/MIP nanocomposites mainly relies on hydroxyl radicals.

To further confirm the •OH, the ESR is performed from which it is evident that a strong ESR signal at g = 2.003 is observed (Fig. S5b), which is indicative of the presence of the hydroxyl radical ($OH^{\cdot}$). The presence of the hydroxyl radical in the N-CNDs/PAni/MIP system suggests its involvement in the oxidation of TMB through peroxidase-like activity. Therefore, the ESR spectra analysis provides valuable information by identifying the hydroxyl radical as a major player in the peroxidase-like activity of the N-CNDs/PAni/MIP system and their role in detecting CIPRO.

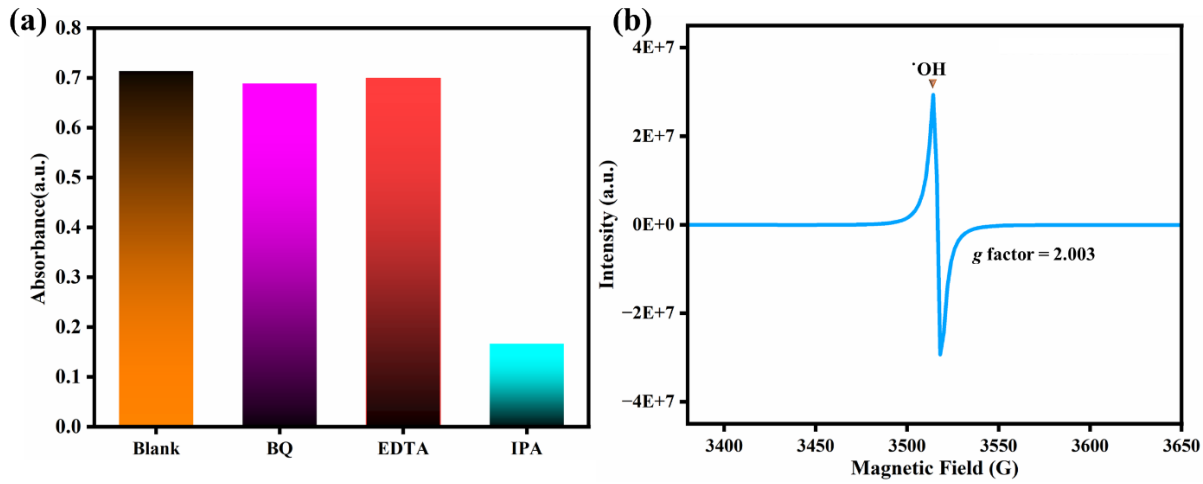

Figure S5. (a) Effect of scavenger and (b) ESR spectra of N-CNDs/PAni/MIP system.

Table S1 Comparison table of the apparent kinetic parameters of N-CNDs/PAni/MIP nanocomposites with different enzyme mimics.

Catalyst	**Substrate**	**Km (mM)**	**V_{max}**	**Reference**
HRP	TMB	0.434	10 (10^{-8} Ms^{-1})	5
	H_2O_2	3.702	8.71 (10^{-8} Ms^{-1})	
CS@GSH-CuNCs	TMB	0.39	1.11 (10^{-7} Ms^{-1})	6
	H_2O_2	27.3	2.53 (10^{-7} Ms^{-1})	
N-CDs	TMB	0.115	2.48 (10^{-8} Ms^{-1})	7
	H_2O_2	0.764	17.15 (10^{8} Ms^{-1})	
N/S CDs	TMB	0.0765	0.3096 (10^{-8} M s^{-1})	8
	H_2O_2	0.0488	0.6799 (10^{-8} Ms^{-1})	
N-CNDs/PAni/MIP	TMB	0.088	0.911 (10^{-8} Ms^{-1})	Present work
	H_2O_2	0.193	1.025 (10^{-8} Ms^{-1})	

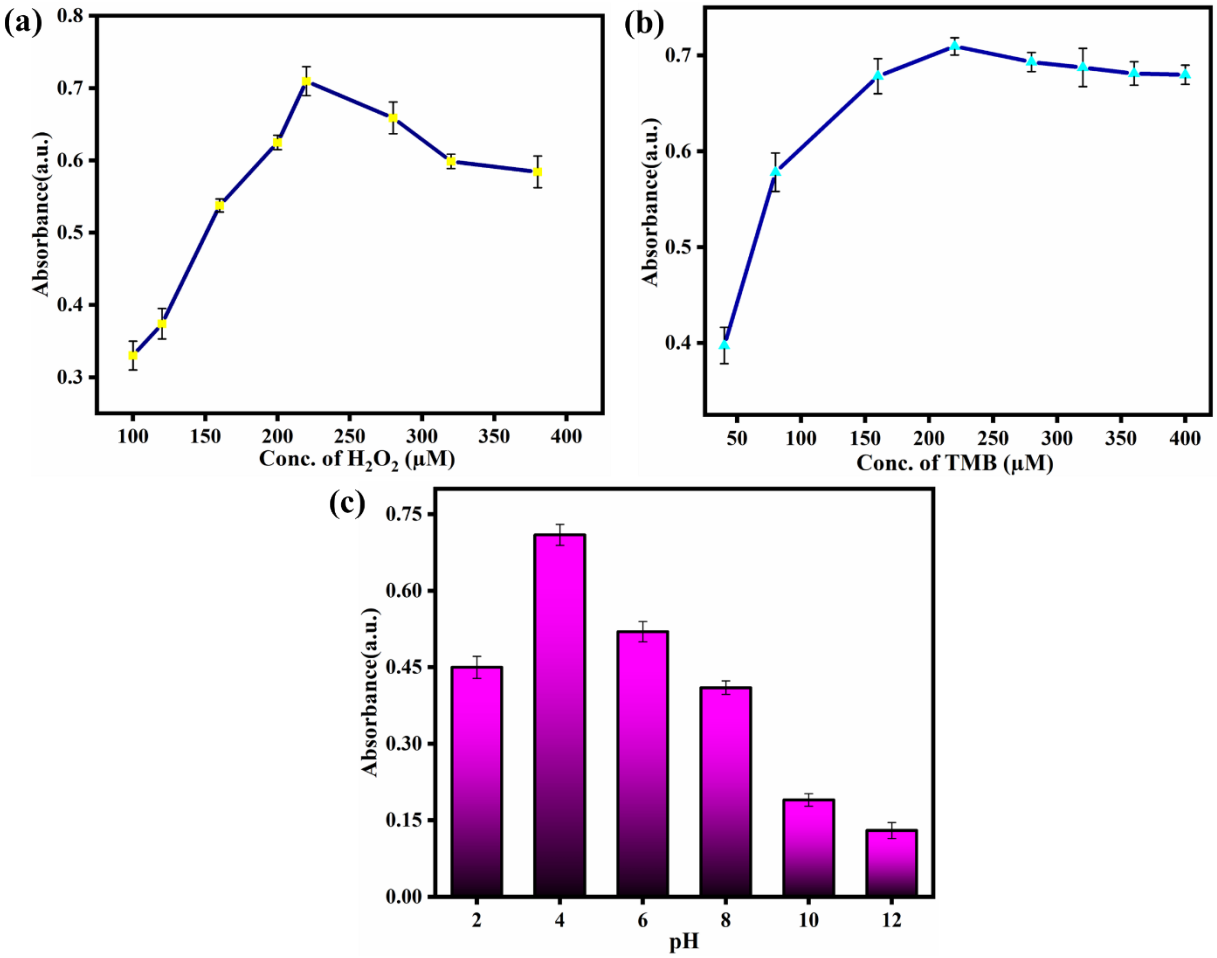

Figure S6. Optimization of (a) concentration of H_2O_2(b) concentration of TMB and (c) incubation of pH

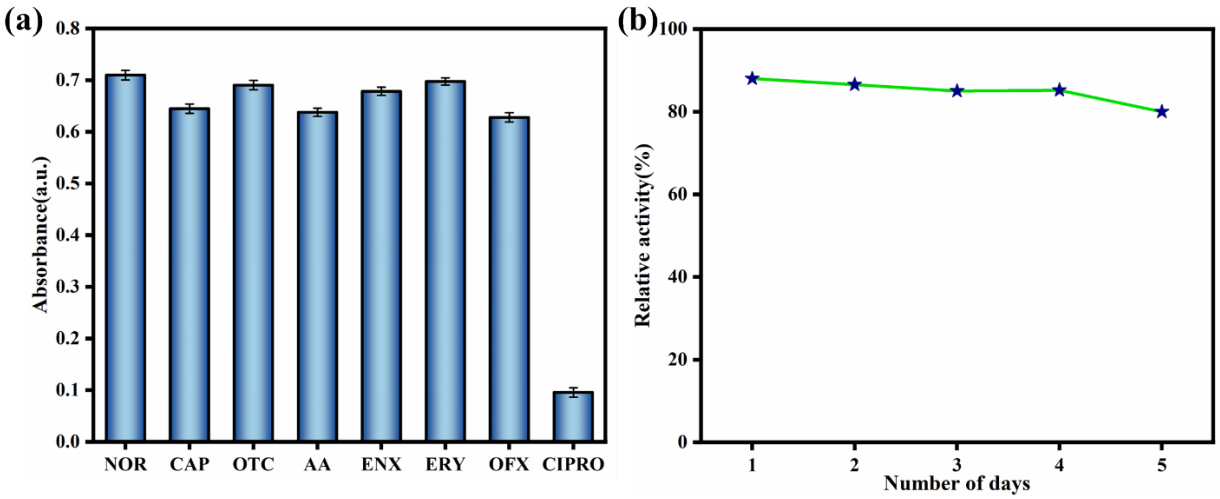

Figure S7. (a) Selectivity of N-CNDs/PAni/MIPs POD-like activity with other analytes. (b) Stability analysis of N-CNDs/PAni/MIPs POD-like activity.

PVA-N-CNDs/PAni/MIP film real sample analysis:

The PVA-N-CNDs/PAni/MIP film that had been prepared was trimmed to a suitable size (0.5x2.0 cm) and subsequently introduced one at a time into water samples containing varying concentrations of CIPRO solution. Next, at a wavelength of 425 nm, the fluorescence intensity of every solution is measured. The detected quantity and recovery of CIPRO have been calculated using the obtained values, and the results are presented in Table S2.

Table S2 Real water sample analysis using PVA-N-CNDs/PAni/MIP film.

Samples	Spiked concentration (nM)	Detected (nM)	Recovery (%)
Pond water	0	0.00 ± 0.00	-
	2	2.02 ± 0.19	101.1
	4	3.99 ± 0.01	99.5
Lake water	0	0.00 ± 0.00	-
	5	4.86 ± 0.89	97.2
	10	10.07 ± 0.25	100.7

References:

1. L. Dennany, P. C. Innis, S. T. McGovern, G. G. Wallace and R. J. Forster, Phys. Chem. Chem. Phys., 2011, 13, 3303–3310.
2. L. Singh and V. Singh, Appl. Phys. A, 2022, 128, 610.
3. T. S. and R. S. D., Appl. Surf. Sci., 2016, 390, 435–443.
4. L. Hu, P. Jiang, P. Zhang, G. Bian, S. Sheng, M. Huang, Y. Bao and J. Xia, J. Mater. Sci., 2016, 51, 8296–8309.
5. R. Zhang and W. Chen, *Biosens. Bioelectron.*, 2014, **55**, 83–90
6. Chen, S., Li, Z., Huang, Z., & Jia, Q., *Sensors and Actuators B: Chemical*, 2021,*332*, 129522.
7. Su, K., Xiang, G., Cui, C., Jiang, X., Sun, Y., Zhao, W., & He, L., *Arabian Journal of Chemistry*, 2023, *16*(3), 104538.

8. Tang, M., Zhu, B., Wang, Y., Wu, H., Chai, F., Qu, F., & Su, Z., *Microchimica Acta*, 2019, 186, 1-14.